

Article

Fractional Growth Model Applied to COVID-19 Data

Fernando Alcántara-López ¹, Carlos Fuentes ^{2,*}, Carlos Chávez ^{3,*}, Fernando Brambila-Paz ¹
and Antonio Quevedo ²

- ¹ Department of Mathematics, Faculty of Science, National Autonomous University of Mexico, Av. Universidad 3000, Circuito Exterior S/N, Delegación Coyoacán 04510, Ciudad de Mexico, Mexico; alcantaralopez@comunidad.unam.mx (F.A.-L.); fernandobrambila@gmail.com (F.B.-P.)
- ² Mexican Institute of Water Technology, Paseo Cuauhnáhuac Núm. 8532, Jiutepec 62550, Mexico; jose_quevedo@tlaloc.imta.mx
- ³ Water Research Center, Department of Irrigation and Drainage Engineering, Autonomous University of Querétaro, Cerro de las Campanas S/N, Col. Las Campanas, Querétaro 76010, Mexico
- * Correspondence: cbfuentesr@gmail.com (C.F.); chagcarlos@uaq.mx (C.C.)

Abstract: Growth models have been widely used to describe behavior in different areas of knowledge; among them the Logistics and Gompertz models, classified as models with a fixed inflection point, have been widely studied and applied. In the present work, a model is proposed that contains these growth models as extreme cases; this model is generalized by including the Caputo-type fractional derivative of order $0 < \beta \leq 1$, resulting in a Fractional Growth Model which could be classified as a growth model with non-fixed inflection point. Moreover, the proposed model is generalized to include multiple sigmoidal behaviors and thereby multiple inflection points. The models developed are applied to describe cumulative confirmed cases of COVID-19 in Mexico, US and Russia, obtaining an excellent adjustment corroborated by a coefficient of determination $R^2 > 0.999$.

Keywords: fractional Caputo derivative; sigmoidal function; Gompertz model; logistic model



Citation: Alcántara-López, F.; Fuentes, C.; Chávez, C.; Brambila-Paz, F.; Quevedo, A. Fractional Growth Model Applied to COVID-19 Data. *Mathematics* **2021**, *9*, 1915. <https://doi.org/10.3390/math9161915>

Academic Editors: Tian-Zhou Xu, Yanshan Zhang, Chun Wang and Bingzhao Li

Received: 13 June 2021
Accepted: 6 August 2021
Published: 11 August 2021

Publisher's Note: MDPI stays neutral with regard to jurisdictional claims in published maps and institutional affiliations.



Copyright: © 2021 by the authors. Licensee MDPI, Basel, Switzerland. This article is an open access article distributed under the terms and conditions of the Creative Commons Attribution (CC BY) license (<https://creativecommons.org/licenses/by/4.0/>).

1. Introduction

Understanding population growth phenomena has been a task that over the time has provided various challenges to mathematicians, physicists, biologists, medics, economists and many others. From economic areas, where applying growth models to poultry allows making imperative predictions for the profitability of operations [1], to biological and medical areas, where growth models have been applied to the growth of animals, plants, yeast cells, tumors and recently to adjust and model COVID-19 pandemic data [2–5].

Several authors classify population growth models as bounded and unbounded, where bounded growth models are characterized by having a sigmoidal behavior with a fixed inflection point or a sigmoidal behavior with a non-fixed inflection point [1,2].

Among the various existing growth models, Logistics (Verhulst) and Gompertz models have been widely studied and solved by a large number of methods; some of which are: successive approximation method, singular perturbation method, Adomian decomposition method, shifted Legendre polynomials, homotopy method, see [5–15] and the references therein; where even fractal dimensions are considered for the case of the Logistics equation.

In order to model phenomena with greater precision, fractional calculus has been implemented in growth models; particularly, in the models previously described. For the Logistic model, it has been implemented in the discrete model showing chaotic fractional behavior and fractional bifurcation diagrams [12]; in the continuous model, the fractional predictor-corrector scheme is implemented [13]; reaching analytical solutions considering power law coefficients [14]; and even conformable derivatives [15], all of these considering the fractional derivative of the Caputo type.

For the Gompertz model, the Caputo-type fractional derivative is implemented in the Gompertz linearized differential equation and solved by means of the Laplace transform [5];

on the other hand, in the linearized Gompertz equation, the Caputo fractional derivative of a function is implemented with respect to the exponential function, allowing the asymptotic behavior of the function to depend on the order of the fractional derivative [11].

In general, solving fractional problems analytically, whether linear or nonlinear, represents a great challenge; therefore, the generalization of numerical methods to approximate fractional derivatives and fractional differential equations has been a very useful tool. When proposing numerical schemes, various authors use the relationship between the Caputo derivative and the Riemann–Liouville derivative where stability and convergence have been fully studied [16]; on the other hand, the equivalence between the derivative of Caputo and the integral equation of Volterra is used, where the stability and convergence have been proven in various works [17–20].

Finally, COVID-19 is a recent disease caused by the SARS-CoV-2 virus and declared as a public health emergency of international importance by the World Health Organization (WHO) on 30 January 2020 [21]; since then, many countries have implemented complex models in order to understand the behavior of this phenomenon and thus be able to make predictions [22–24]; even for these arduous modeling tasks, models as simple as Logistics and Gompertz continue to be used, showing a good fit to describe cumulative data on confirmed cases and deaths [3,4,25].

The work proceeds as follows. Section 2 shows the necessary tools of Fractional Calculus. Section 3 develops the fractional growth model while Section 4 justifies the existence and uniqueness of the solution of the model with the numerical scheme applied. Section 5 generalizes the model to include multiple sigmoidal behaviors and, therefore, multiple inflection points. In Section 6, the models developed are applied to describe the data of COVID-19 cases from Mexico, US and Russia. Finally, Section 7 summarizes the results shown and the conclusions reached.

2. Fractional Calculus

To model phenomena with physical initial conditions, the Caputo fractional derivative is naturally the choice to make. Next, this fractional derivative will be defined along with some of its most important properties, for more information, see [26,27].

Definition 1. Let $-\infty < t_0 < \infty$. The Riemann–Liouville fractional integral, ${}^{RL}I_{t_0+}^\beta y(t)$, of order $\beta \in \mathbb{R}$ is defined by

$$\left({}^{RL}I_{t_0+}^\beta y\right)(t) = \frac{1}{\Gamma(\beta)} \int_{t_0}^t (t-\tau)^{\beta-1} y(\tau) d\tau, \quad t > t_0, \quad (1)$$

where $\Gamma(\cdot)$ is Euler's gamma function.

From the fractional integral, we have to definitions.

Definition 2. The Riemann–Liouville fractional derivative, ${}^{RL}D_{t_0+}^\beta y(t)$, of order $\beta \in \mathbb{R}$ is defined by

$$\left({}^{RL}D_{t_0+}^\beta y\right)(t) = \left(\frac{d^n}{dt^n} {}^{RL}I_{t_0+}^{n-\beta} y\right)(t) = \frac{1}{\Gamma(n-\beta)} \frac{d^n}{dt^n} \int_{t_0}^t (t-\tau)^{n-\beta-1} y(\tau) d\tau, \quad (2)$$

where $n \in \mathbb{N}$ with $n-1 < \beta \leq n$.

Definition 3. The Caputo fractional derivative, ${}^CD_{t_0+}^\beta y(t)$, of order $\beta \in \mathbb{R}$, is defined by

$$\left({}^CD_{t_0+}^\beta y\right)(t) = \left({}^{RL}I_{t_0+}^{n-\beta} \frac{d^n}{dt^n} y\right)(t) = \frac{1}{\Gamma(n-\beta)} \int_{t_0}^t (t-\tau)^{n-\beta-1} y^{(n)}(\tau) d\tau, \quad (3)$$

where $n \in \mathbb{N}$ with $n-1 < \beta \leq n$ and $y^{(n)}$ is the n -th derivative.

The Riemann–Liouville fractional derivative and Caputo fractional derivative are related by

$$({}^C D_{t_0+}^\beta y)(t) = \left({}^{RL} D_{t_0+}^\beta \left[y(x) - \sum_{j=0}^{n-1} \frac{y^{(j)}(t_0)}{j!} (x - t_0)^j \right] \right)(t). \tag{4}$$

Although both definitions of fractional derivative are strongly related, they have great differences such as their behavior for constants, that is, if $y(t) = c$ with c a constant, then

$$({}^{RL} D_{t_0+}^\beta y)(t) = \frac{c(t - t_0)^{-\beta}}{\Gamma(1 - \beta)}; \tag{5}$$

$$({}^C D_{t_0+}^\beta y)(t) = 0; \tag{6}$$

furthermore, when considering applications, the Caputo fractional derivative allows us to continue using initial conditions as in the classical case, with integer derivatives, which is not the case for the Riemann–Liouville fractional derivative.

3. Fractional Growth Model

Definition 4. Logistic and Gompertz growth models are defined, respectively, through the following differential equations:

$$\frac{dN}{dt} = rN(t) \left(1 - \frac{N(t)}{N_\infty} \right), \quad N(0) = N_0; \tag{7}$$

$$\frac{dN}{dt} = rN(t) \ln \left(\frac{N_\infty}{N(t)} \right), \quad N(0) = N_0; \tag{8}$$

where $N = N(t)$ represents the size of the population, t is time, $r > 0$ is the growth rate, $N_\infty > 0$ is the maximum number of individuals that the population can sustain or carrying capacity of the environment and N_0 is the initial condition.

Indeed, Logistic and Gompertz growth models have been studied extensively and both are classified as models with a fixed inflection point where the inflection point in each model is given, respectively, by

$$N_{\text{inflection}} = \frac{N_\infty}{2}, \quad \text{in} \quad t_{\text{inflection}} = \frac{1}{r} \ln \left(\frac{N_\infty}{N_0} - 1 \right); \tag{9}$$

$$N_{\text{inflection}} = \frac{N_\infty}{e}, \quad \text{in} \quad t_{\text{inflection}} = \frac{1}{r} \ln \left(\ln \left(\frac{N_\infty}{N_0} \right) \right). \tag{10}$$

Considering the limit

$$\lim_{\mu \rightarrow \infty} \mu \left(1 - x^{1/\mu} \right) = -\ln(x), \tag{11}$$

and substituting the integer derivative for the Caputo fractional derivative, Logistic and Gompertz models, Equations (7) and (8), can be generalized by the following fractional growth model; namely

$${}^C D_0^\beta N(t) = r\mu N(t) \left(1 - \left(\frac{N(t)}{N_\infty} \right)^{1/\mu} \right), \quad N(0) = N_0; \tag{12}$$

where $N(t)$, N_∞ and t have the same meaning as in Equations (7) and (8) and $\mu > 0$ is a shape parameter; while $r = \nu/\tau^{\beta-1}$ where ν is a growth rate and τ is a reference time introduced in order to maintain dimensional balance in the equation. Note that for $\beta = 1$ and $\mu = 1$, the fractional model becomes the Logistic model and, for $\mu \rightarrow \infty$, the model

is equivalent to the Gompertz model. Likewise, for the non-fractional case, $\beta = 1$, the inflection point is

$$N_{\text{inflection}} = \frac{N_{\infty}}{(1 + 1/\mu)^{\mu}}, \quad \text{in} \quad t_{\text{inflection}} = \frac{1}{r} \ln \left(\mu \left[\left(\frac{N_{\infty}}{N_0} \right)^{1/\mu} - 1 \right] \right); \quad (13)$$

where it is concluded that the fractional model, even for $\beta = 1$, belongs to the family of growth models with a non-fixed inflection point.

4. Analytical and Numerical Solution of the Fractional Growth Model

Equation (12) shows the model studied in this work. Before showing the results of the fractional growth model and its application, some results on the existence and uniqueness of the solution of the fractional growth model as well as the numerical scheme used will be shown.

4.1. Existence and Uniqueness of Solutions

Let

$$f(t, N(t)) = r\mu N(t) \left(1 - \left(\frac{N(t)}{N_{\infty}} \right)^{1/\mu} \right), \quad (14)$$

be the right part of the fractional differential Equation (12); consider the following theorems given by Diethelm and Ford [28].

Theorem 1 (Existence). Assume that $\mathcal{D} := [0, \chi^*] \times [N_0 - \alpha, N_0 + \alpha]$ with some $\chi^* > 0$ and some $\alpha > 0$, and let the function $f : \mathcal{D} \rightarrow \mathbb{R}$ be continuous. Furthermore, define $\chi := \min\{\chi^*, (\alpha\Gamma(\beta + 1) / \|f\|_{\infty})^{1/\beta}\}$. Then, there exists a function $N : [0, \chi] \rightarrow \mathbb{R}$ solving the initial value problem (12).

Theorem 2 (Uniqueness). Assume that $\mathcal{D} := [0, \chi^*] \times [N_0 - \alpha, N_0 + \alpha]$ with some $\chi^* > 0$ and some $\alpha > 0$. Furthermore, let the function $f : \mathcal{D} \rightarrow \mathbb{R}$ be bounded on \mathcal{D} and fulfill a Lipschitz condition with respect to second variable, i.e.,

$$|f(t, y) - f(t, z)| \leq L|y - z| \quad (15)$$

with some constant $L > 0$ independent of t, y and z . Then, denoting χ as in Theorem 1, there exists at most one function $N : [0, \chi] \rightarrow \mathbb{R}$ solving the initial value problem (12).

Indeed, the function shown in Equation (14) satisfies the conditions required by the theorems given by Diethelm and Ford, so it is concluded that the solution of the fractional growth model, Equation (12), exists and is unique.

4.2. Stability and Numerical Convergence

Let $t \in [0, T]$ with $T > 0$ and consider a uniform mesh with the nodes defined by $t_k = k\Delta t$ with $\Delta t = T/n$ and $k = 0, 1, \dots, n$.

Note that the fractional growth model, Equation (12), is equivalent to the Volterra integral equation

$$N(t) = N_0 + \frac{1}{\Gamma(\beta)} \int_0^t (t - s)^{\beta-1} f(s, N(s)) ds, \quad (16)$$

where f is as in Equation (14).

Considering Euler’s fractional method, the numerical scheme applied is

$$N(t_{k+1}) = N_0 + \frac{1}{\Gamma(\beta)} \sum_{j=0}^k b_{j,k+1} f(t_j, f(N(t_j))) \quad (17)$$

with $b_{j,k+1} = \frac{\Delta t^\beta}{\beta} [(k-j+1)^\beta - (k-j)^\beta]$ where $0 \leq j \leq k$ and $k = 0, 1, \dots, n-1$. The numerical stability of this method has been extensively studied for both linear and nonlinear fractional differential equations, see [29,30] and the references therein.

4.3. Sensitivity Analysis

Next, we will show synthetic results of the fractional growth model and its sensitivity to the variation of the main parameters of the model, namely μ and β .

Figures 1 and 2 show the numerical results of the fractional growth model for $0 < \beta \leq 1$ considering the numerical scheme shown in Equation (17). Figure 1 shows the case $\beta = 1$, where the fractional growth model recovers the extreme behaviors of the Logistics model and Gompertz model by varying the parameter μ ; Figure 1a shows the behavior of the function $N(t)$; while Figure 1b shows the behavior of the function $N'(t)$ that shows how the inflection point moves as function of the parameter μ .

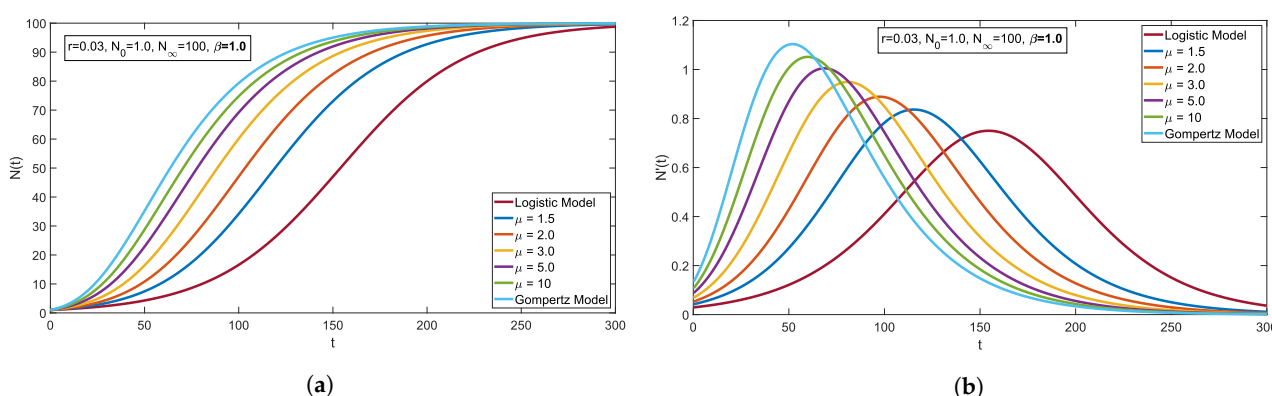


Figure 1. Fractional Growth Model and its derivative with the classic fractional derivative order, $\beta = 1$, varying the parameter μ where the classical sigmoidal behavior and its non-fixed inflection point are shown. (a) Fractional Growth Model by varying the parameter μ . (b) Derivative of the Fractional Growth Model by varying the parameter μ .

Figure 2 shows the behavior of the fractional growth model with different values of the order of the fractional derivative β . For $\beta = 1$, the fractional derivative behaves as the classical derivative. Figure 2a shows the sigmoidal behavior of the function $N(t)$, while Figure 2b shows the behavior of its derivative where the inflection point varies, also, as a function of β .

Figure 2 shows that when the order of the fractional derivative β decreases, the sigmoidal behavior of the function is lengthened, delaying the appearance of the inflection point. It is also observed how the asymptotic behavior of the function is affected, showing not only a slower growth, it is also shown that the asymptote reached is smaller as $\beta \rightarrow 0$.

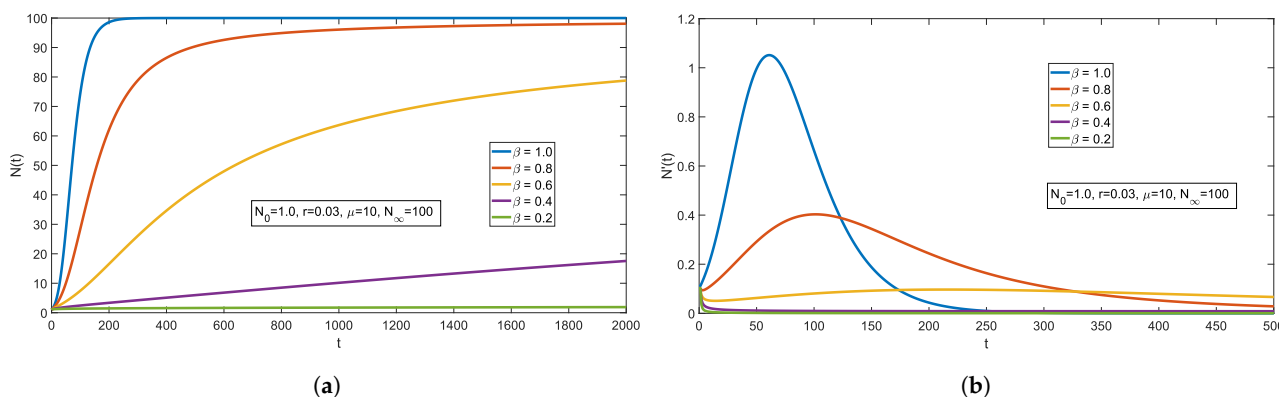


Figure 2. Fractional Growth Model and its derivative varying the order of the fractional derivative β where the sigmoidal behavior and its non-fixed inflection point are preserved. (a) Fractional growth model varying the order of the fractional derivative β . (b) Derivative of the Fractional Growth Model by varying the order of the fractional derivative β .

5. Fractional Growth Model for Sprouts

Growth models, including the fractional growth model, Equation (12), have the characteristic of having a single sigmoidal behavior, that is, a single inflection point. In order to describe growth data with multiple sigmoidal behaviors and therefore multiple inflection points, the fractional growth model will be generalized.

Suppose a growth phenomenon with k sprouts; because the number of individuals is clearly additive, the principle of superposition will be applied and the global phenomenon will be modeled as the sum of each local phenomenon, namely

$$N(t) = \sum_{j=1}^k N_j(t), \tag{18}$$

where $N_j(t)$ for $j = 0, 1, \dots, k$ satisfies Equation (12) with its respective parameters.

The global initial condition, N_0 , and the global maximum number of individuals that the population can sustain, N_∞ , are defined as

$$N_0 = \sum_{j=1}^k N_{j,0}, \quad N_\infty = \sum_{j=1}^k N_{j,\infty}; \tag{19}$$

where $N_{j,0}$ and $N_{j,\infty}$ are the initial condition and the maximum number of individuals that the population can sustain for each sprout.

Let the weight factors ω_j be given as

$$\omega_j = \frac{N_{j,0}}{N_0} = \frac{N_{j,\infty}}{N_\infty}; \tag{20}$$

clearly, it is true that $\sum_{j=1}^k \omega_j = 1$.

Therefore, the fractional growth model with multiple sprouts is

$${}^C D_0^\beta N(t) = \sum_{j=1}^k {}^C D_0^{\beta_j} N_j(t) = \sum_{j=1}^k r_j \mu_j N_j(t) \left(1 - \left(\frac{N_j(t)}{\omega_j N_\infty} \right)^{1/\mu_j} \right), \quad N(0) = N_0. \tag{21}$$

The numerical scheme applied to solve the fractional growth model for multiple sprouts, Equation (21), was obtained analogously to the numerical scheme shown in Equation (17), that is,

$$N(t_{m+1}) = \sum_{j=1}^k N_j(t_{m+1}) = N_0 + \sum_{j=1}^k \frac{1}{\Gamma(\beta_j)} \sum_{l=0}^m b_{l,m+1} r_j \mu_j N_j(t_m) \left(1 - \left(\frac{N_j(t_m)}{\omega_j N_\infty} \right)^{1/\mu_j} \right). \tag{22}$$

The proof for the existence and uniqueness for the fractional growth model with multiple sprouts as well as the numerical stability of the used scheme are proven by induction without much effort, so it will be omitted for reasons of space.

The fractional growth model with multiple sprouts, Equation (21), was solved numerically by applying the numerical scheme shown in Equation (22). In order for the function $N(t)$ to be a solution of the fractional growth model with multiple sprouts and to fit cumulative confirmed case data of COVID-19, the function fit from MATLAB was applied to find the values of the parameters in the model.

6. Applications to COVID-19 Data

Since the beginning of the pandemic, the effect of COVID-19 has been different throughout the world; however, even with the various measures that each country has taken, the accumulated confirmed cases continue to have a sigmoidal behavior. Therefore, the fractional growth model will be applied to describe the cumulative confirmed cases of COVID-19 from Mexico, the United States (US) and Russia during their first outbreak and

the fractional growth model with multiple sprouts will be applied to all the data obtained from their respective first case to 14 July 2021 [31].

6.1. Mexico Data

Historically, the first confirmed case of COVID-19 in Mexico was on 28 February 2020 [32]; Mexico has constantly updated, through its official pages, the number of Confirmed, Suspect, Negative and Deaths caused throughout the pandemic [31,33].

Figure 3 shows the confirmed cases data of COVID-19 from 28 January 2020 to 14 July 2021; where cumulative confirmed cases are shown in red, while daily confirmed cases are shown in blue.

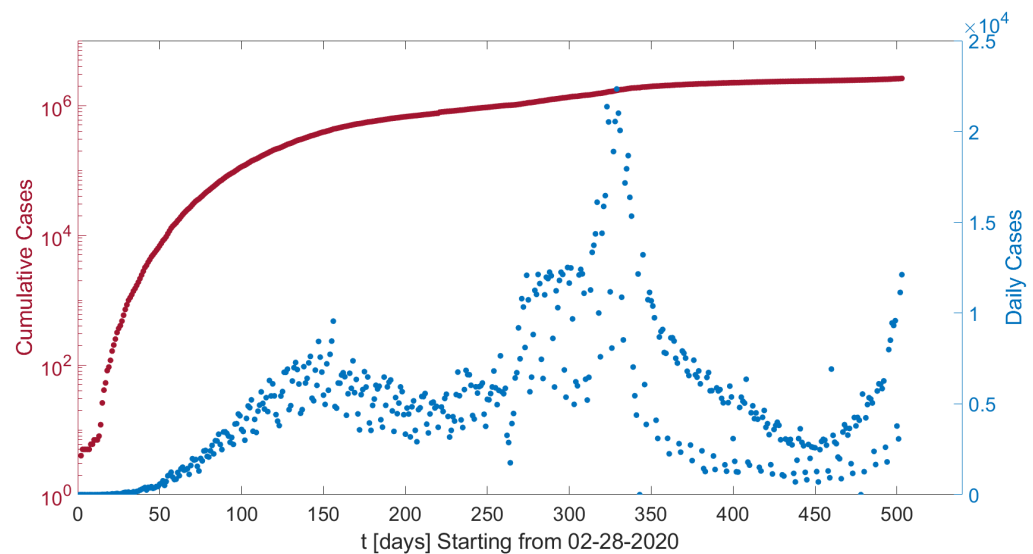


Figure 3. COVID-19 Mexico data.

For the purpose of applying both models, the fractional growth model and the fractional growth model with multiple sprouts, different datasets will be considered for each model and the Matlab function fit will be applied to find the corresponding parameters that minimize the error in the least squares sense.

6.1.1. Fractional Growth Model with One Sprout

In order to adequately describe the data presented by the proposed fractional growth model, the data will be taken from 1 March 2020 to 1 October 2020; because from the proposed initial date, it is observed that cumulative cases have an exponential growth type behavior and, after the proposed final date, the effect of a subsequent sprout is observed.

Figure 4 shows the fit made by the fractional growth model, Equation (12), to the proposed data corresponding to the observed 1st wave of COVID-19. Figure 4a shows the comparison between the model and the cumulative confirmed cases on a semilog scale where it is observed that from a certain day, $t \approx 70$ days, there is no distinction between the model and the data. Figure 4b shows the comparison between $N'(t)$, calculated numerically from the numerical solution obtained, and the confirmed daily cases where, despite the dispersion shown by the daily cases data, a very good fit is observed by the model which is corroborated by the coefficient of determination R^2 , as observed in Table 1.

From the fitted parameters it is observed that, because $\mu \gg 1$, the Fractional Growth Model has a similar Gompertz-like behavior; furthermore, because $\beta < 1$, the phenomenon shows a slower growth compared to a classical growth with integer derivative. Likewise, the model shows its inflection point at $t = 146.3$ while the day of maximum confirmed cases was reported on 1 August 2020, that is, $t = 154$.

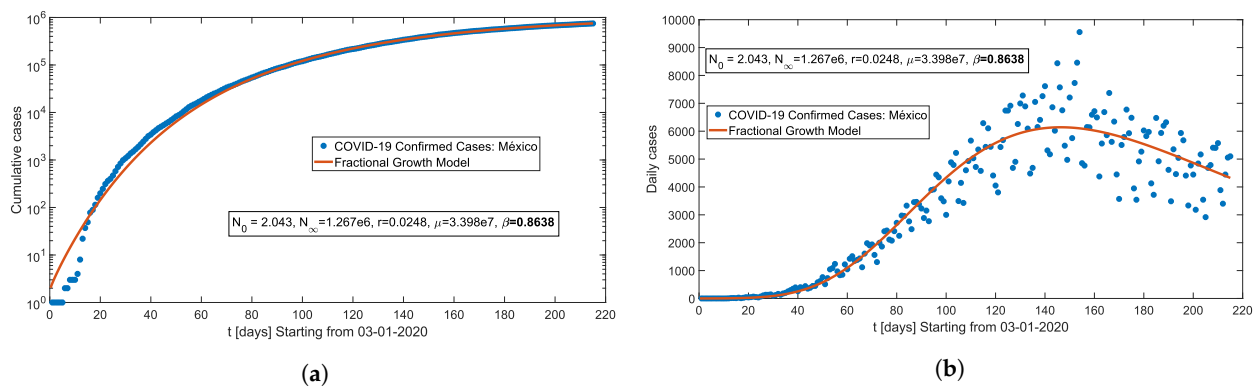


Figure 4. Fractional Growth Model Fit for single sprout compared to confirmed COVID-19 data from Mexico. In (a) the function $N(t)$, solution to the fractional growth model, is compared with the cumulative confirmed cases; while in (b) the function $N'(t)$ is compared with the confirmed daily cases.

6.1.2. Fractional Growth Model with Multiple Sprouts

Consider the data from 1 March 2020 to 14 July 2021 and consider the fractional growth model for multiple sprouts, Equation (21). Figure 5 shows the fit made by the fractional growth model with multiple sprouts, with $k = 3$, to the cumulative confirmed data of COVID-19 in Mexico.

Figure 5a shows the fit from the model for $k = 3$ sprouts compared to the cumulative confirmed cases on logarithmic scale. Although, at the beginning, there is a slight difference between the data and the adjustment carried out, it is observed that after a certain day, $t \approx 70$ days, the difference is indistinguishable. On the other hand, Figure 5b shows the comparison between $N'(t)$, calculated numerically, and the confirmed daily cases where, as can be seen, the behavior of the model follows the characteristic behavior of the data, that is, it shows a good concordance between the inflection points of the model and the moments of maximum recorded cases, as well as the increasing and decreasing behaviors which is shown by the R^2 , as observed in Table 1.

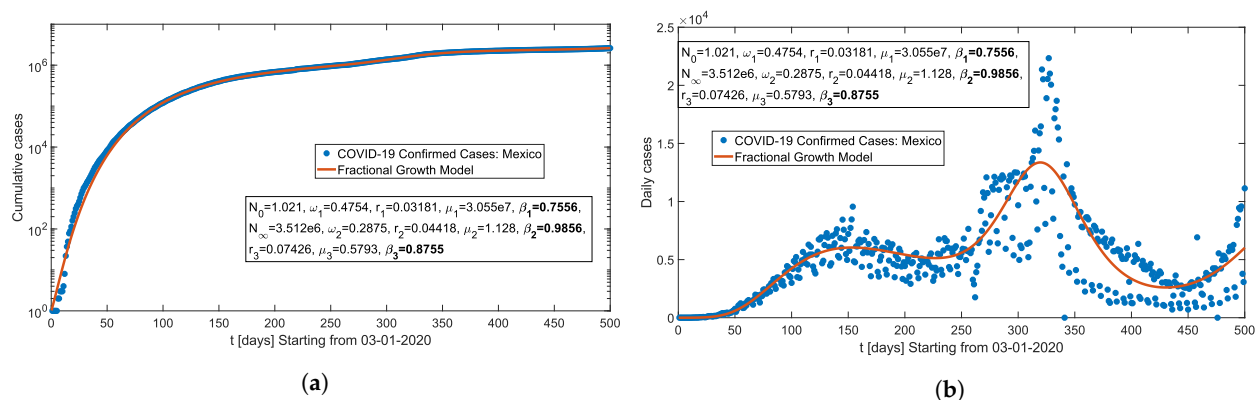


Figure 5. Fractional Growth Model Fit for $k = 3$ sprouts compared to confirmed COVID-19 data from Mexico. In (a) the function $N(t)$, solution to the fractional growth model with multiple sprouts, is compared with the cumulative confirmed cases; while in (b) the function $N'(t)$ is compared with the confirmed daily cases.

Figure 5 shows 2 sprouts already finished and a third sprout in process, where the first outbreak had a considerably longer duration than the subsequent sprouts, $\omega_1 = 0.4754$; likewise, $\mu_1 \gg 1$ implies that the first outbreak has a Gompertz-like behavior while the following sprouts have a Logistic-like behavior.

Note that, by applying the principle of superposition, that is, when considering each sprout as part of a global phenomenon, the parameters that characterize each sprout are susceptible to global behavior, which explains why the parameters shown in Figure 5 for the first sprout do not match those shown in Figure 4.

Finally, observing the order of the fractional derivative for each sprout, β_i for $i = 1, 2, 3$; the first sprout had a considerably slower behavior than a classical behavior with an integer derivative and, therefore, a delay in the appearance of the maximum number of confirmed cases, that is, the inflection point; the second sprout, given that $\beta_2 \approx 1$, has a behavior very close to the classical behavior with integer derivative, so the delay in this case is little; for the third sprout, considering the fit with the actual data, a considerably slower development is observed than could be obtained for a classical behavior with an integer derivative.

6.2. US Data

The reported data of confirmed cases by COVID-19 in the US date back to 22 January 2020 [31]. In this time period, the data have proven that the US has had multiple sprouts of COVID-19; therefore, the fractional growth model for multiple sprouts will be applied directly to the full history data.

Figure 6 shows the confirmed cases of COVID-19 from 22 January 2020 to 14 July 2021; where cumulative confirmed cases are shown in red while daily confirmed cases are shown in blue.

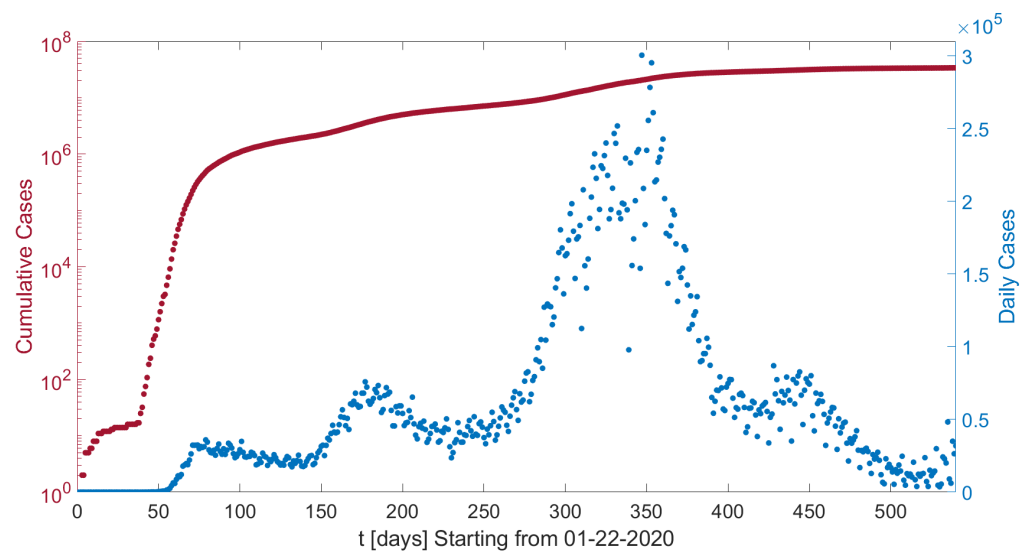


Figure 6. COVID-19 US data.

Figure 7 shows the fit made by the fractional growth model with $k = 4$ sprouts to the cumulative confirmed data of COVID-19 in the US since 13 March 2020. This is because, from this date, the cumulative data begin to show an exponential growth type behavior.

Figure 7a shows the comparison between the fit made by the model and the cumulative confirmed data on a logarithmic scale where from a certain day, $t \approx 40$, there is no visual distinction between the model and the data. Figure 7b shows the comparison between $N'(t)$, calculated numerically, and the confirmed daily cases where it is observed that, despite the dispersion in the data, the model has a good fit, which is corroborated by the coefficient of determination R^2 in Table 1.

Based on the parameters shown in Figure 7, the first and second sprouts have had a similar duration, $\omega_1 \approx 0.14 \approx \omega_2$, and the third sprout has had a noticeably longer duration, $\omega_3 \approx 0.6$; likewise, the first sprout has a Gompertz-like behavior, $\mu_1 \gg 1$, while the subsequent sprouts has a Logistic-like behavior, $\mu_k \approx 1$ for $k = 2, 3, 4$.

It is remarkable to observe that, since the order of the fractional derivative associated with the first two sprouts, β_1 and β_2 , is less than one, the behavior in both sprouts is considerably slower compared to the classical behavior with integer derivative, that is, the time of maximum daily cases was substantially delayed and, at the same time, the number of maximum cases also decreased. On the other hand, the third sprout shows a value of β_3 near to 1 which implies that this sprout had an almost classical behavior; finally, the fourth

sprout shows a value of $\beta_4 \approx 0.9$ showing that this sprout is slower than what could be observed with a classic case, although not on a par with the first sprouts.

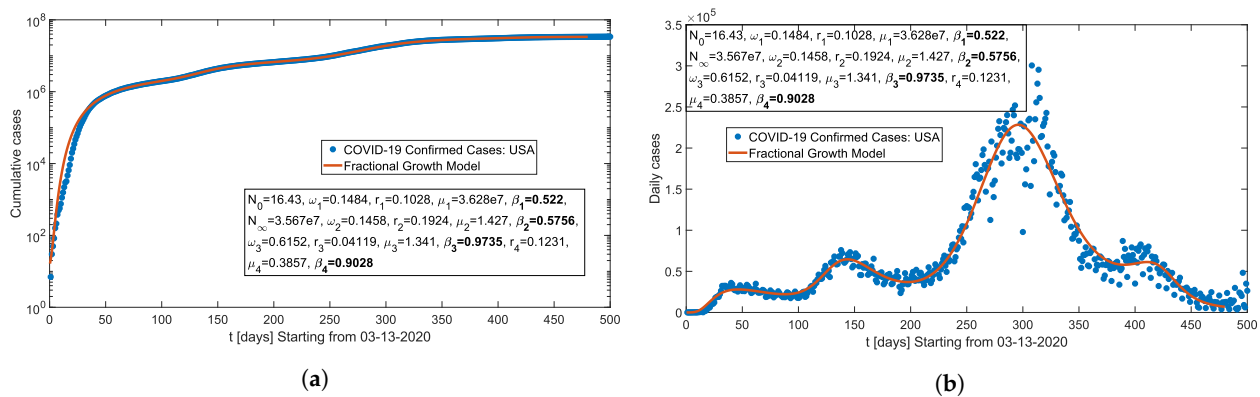


Figure 7. Fractional Growth Model Fit for $k = 4$ sprouts compared to confirmed COVID-19 data from the US. In (a) the function $N(t)$, solution to the fractional growth model with multiple sprouts, is compared with the cumulative confirmed cases; while in (b) the function $N'(t)$ is compared with the confirmed daily cases.

6.3. Russia Data

The reported data of confirmed cases by COVID-19 in Russia date back to 31 January 2020, [31]. Since then and until 14 July 2021, COVID-19 has shown multiple sprouts in the country. Figure 8 shows these data where cumulative confirmed cases are shown in red while daily cases are shown in blue.

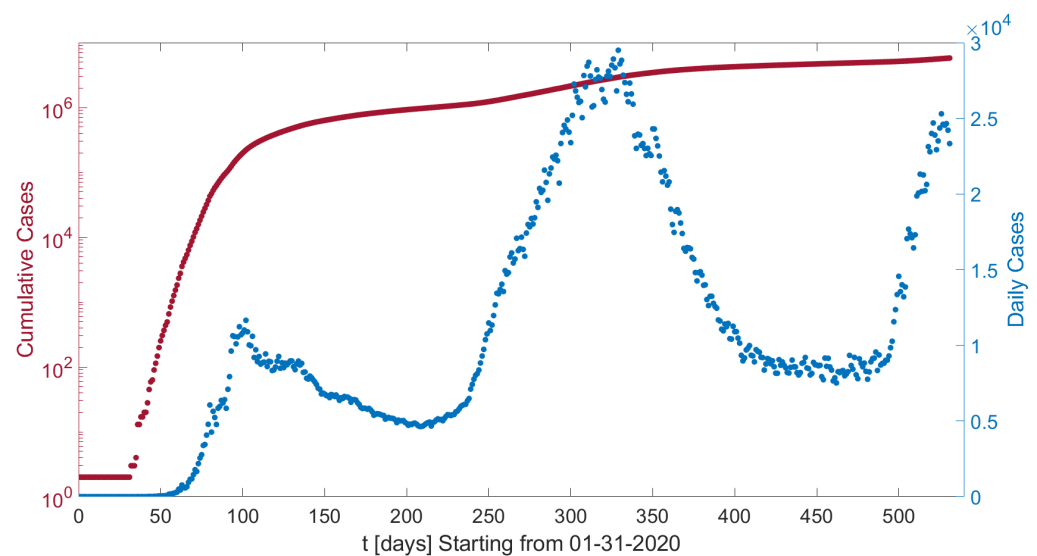


Figure 8. COVID-19 Russia data.

Figure 9 shows the fit made by the fractional growth model with $k = 3$ sprouts to the data of cumulative confirmed cases since March 13, 2020, since from this date, an exponential growth is observed.

Figure 9a compares the model with the cumulative confirmed cases on a logarithmic scale, while Figure 9b compares the function $N'(t)$, calculated numerically, with the confirmed daily cases, where a low data dispersion is observed which allows an excellent fit by the model, verified by the coefficient of determination R^2 , Table 1.

Considering the data shown in Figure 9, there are 2 finished sprouts and a third sprout in development in Russia. The first sprout has a Gompertz-like behavior, $\mu_1 \gg 1$, while the following sprouts have a Logistic-like behavior, $\mu_k \approx 1$ for $k = 2, 3$; it is observed that the second sprout lasts considerably longer than the first sprout $\omega_2 \approx 0.5$.

In this case, it is observed from the order of the fractional derivative that the first sprout has a slower behavior compared to how it would appear if said sprout had a classical behavior with an integer derivative; while for the second sprout, even though there is indeed a slight slowdown in the phenomenon, the behavior is similar to the classical case.

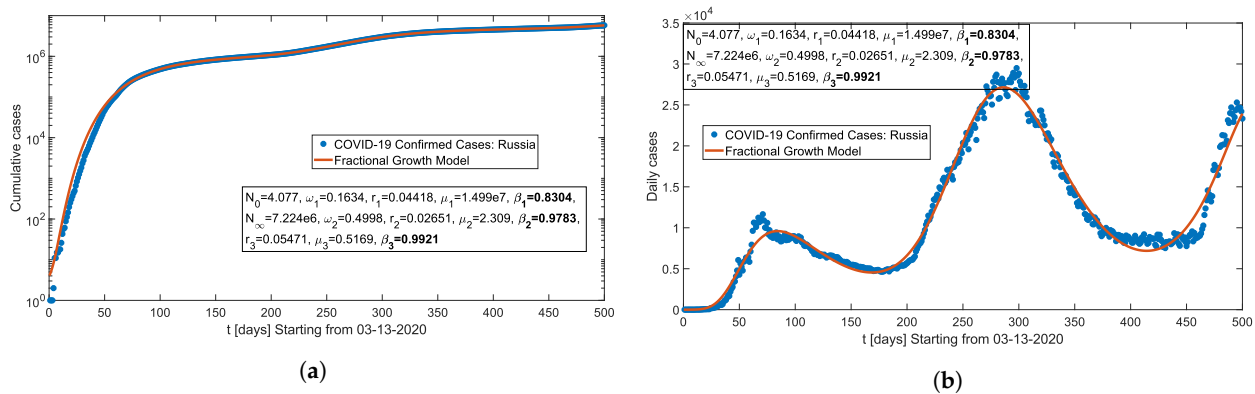


Figure 9. Fractional Growth Model Fit for $k = 3$ sprouts compared to confirmed COVID-19 data from Russia. In (a) the function $N(t)$, solution to the fractional growth model with multiple sprouts, is compared with the cumulative confirmed cases; while in (b) the function $N'(t)$ is compared with the confirmed daily cases.

Table 1. Statistical results of the fit of the Fractional Growth Model and the Fractional Growth Model for multiple sprouts.

Country	Model	R^2	Forecast Peak	Real Peak
Mexico	Single Sprout	0.9998	$t = 146.3$ days	$t = 154$ days
	Multiple Sprouts	0.9999	$t = 153.3$ and $t = 319.7$ days	$t = 154$ and $t = 327$ days
US	Multiple Sprouts	0.9999	$t = 46.7$, $t = 143.7$, $t = 296$ and $t = 410.7$ days	$t = 40$, $t = 138$, $t = 308$ and $t = 389$ days
Russia	Multiple Sprouts	0.99996	$t = 84$ and $t = 286.3$ days	$t = 71$ and $t = 298$ days

Finally, Table 1 shows a summary of the adjustments made by the fractional growth model for a single sprout and for multiple sprouts to the data of cumulative confirmed cases by COVID-19 in Mexico, US and Russia. It is observed that, in effect, the adjustments are excellent given that, for all the applications, the coefficient of determination R^2 is greater than 0.999. Furthermore, the inflection points by the models are shown in comparison with the number of the day with the maximum number of confirmed registered cases, where it is observed that, in general, the days obtained by the model are quite close to the real data.

7. Conclusions

A growth model is proposed that contains the Gompertz and Logistics models as particular cases. The Caputo fractional derivative was incorporated with $0 < \beta \leq 1$ obtaining the fractional growth model which belongs to the class of models with non-fixed inflection point. Furthermore, in order to apply the model to phenomena with multiple sigmoidal growths and, therefore, with multiple inflection points, the proposed model was generalized to obtain a fractional growth model for multiple sprouts. The models developed were applied to describe cumulative confirmed cases of COVID-19 in Mexico, US and Russia, obtaining excellent adjustments corroborated by the coefficient of determination, R^2 , where for all the adjustments made, it was obtained that $R^2 > 0.999$. Finally, it was shown how the different sprouts in the various countries have behaviors similar to the Gompertz and Logistics models and how these sprouts were far from having a classic behavior, with an integer derivative, which can be considered as a consequence of the measures taken by these countries. The models developed, even when they were applied for $0 < \beta \leq 1$, can also describe sigmoidal behaviors that have a more aggressive or fast-spreading behavior, as is the case of some COVID-19 strains that are currently spreading.

Author Contributions: All authors contributed equally to this work. All authors have read and agreed to the published version of the manuscript.

Funding: The first author is grateful to CONACYT for the scholarship grant, scholarship number 548429. Additionally, the UNAM PAPIIT program is thanked for its support.

Institutional Review Board Statement: Not applicable.

Informed Consent Statement: Not applicable.

Data Availability Statement: Publicly available datasets were analyzed in this study. This data can be found here: <https://coronavirus.jhu.edu>, accessed on 18 May 2021.

Conflicts of Interest: The authors declare no conflicts of interest.

References

1. Kuhi, H.D.; Porter, T.; López, S.; Kebreab, E.; Strathe, A.; Dumas, A.; Dijkstra, J.; France, J. A review of mathematical functions for the analysis of growth in poultry. *World's Poult. Sci. J.* **2010**, *66*, 227–240. [CrossRef]
2. Divya, B.; Kavitha, K. A Review on Mathematical Modelling in Biology and Medicine. *Adv. Math. Sci. J.* **2020**, *9*, 5869–5879. [CrossRef]
3. Medina-Mendieta, J.F.; Cortés-Cortés, M.; Cortés-Iglesias, M. COVID-19 Forecasts for Cuba Using Logistic Regression and Gompertz Curves. *MEDICC Rev.* **2020**, *22*, 32. [CrossRef] [PubMed]
4. Husniah, H.; Supriatna, A.K. Modified Verhulst Logistic Growth Model Applied to COVID-19 Data in Indonesia as One Example of Model Refinement in Teaching Mathematical Modeling. In 2nd African International Conference on Industrial Engineering and Operations Management, IEOM 2020. 2020. Available online: <https://pesquisa.bvsalud.org/global-literature-on-novel-coronavirus-2019-ncov/resource/pt/covidwho-1232827> (accessed on 18 May 2021)
5. Bolton, L.; Clout, A.H.J.J.; Schoombie, S.W.; Slabbert, J.P. A proposed fractional-order Gompertz model and its application to tumour growth data. *Math. Med. Biol. J. IMA* **2014**, *32*, 187–209. [CrossRef]
6. Golmankhaneh, A.K.; Cattani, C. Fractal Logistic Equation. *Fractal Fract.* **2019**, *3*, 41. [CrossRef]
7. Xu, H. Analytical approximations for a population growth model with fractional order. *Commun. Nonlinear Sci. Numer. Simul.* **2009**, *14*, 1978–1983. [CrossRef]
8. Krishnaveni, K.; Kannan, K.; Balachandar, S. Approximate analytical solution for fractional population growth model. *Int. J. Eng. Technol.* **2013**, *5*, 2832–2836.
9. Markov, S.M. Reaction networks reveal new links between Gompertz and Verhulst growth functions. *BIOMATH* **2019**, *8*, 1904167. [CrossRef]
10. Suansook, Y.; Paithoonwattanakij, K. Dynamic of logistic model at fractional order. In Proceedings of the 2009 IEEE International Symposium on Industrial Electronics, Seoul, Korea, 5–8 July 2009. [CrossRef]
11. Frunzo, L.; Garra, R.; Giusti, A.; Luongo, V. Modeling biological systems with an improved fractional Gompertz law. *Commun. Nonlinear Sci. Numer. Simul.* **2019**, *74*, 260–267. [CrossRef]
12. Wu, G.C.; Baleanu, D. Discrete fractional logistic map and its chaos. *Nonlinear Dyn.* **2013**, *75*, 283–287. [CrossRef]
13. El-Sayed, A.; El-Mesiry, A.; El-Saka, H. On the fractional-order logistic equation. *Appl. Math. Lett.* **2007**, *20*, 817–823. [CrossRef]
14. Tarasov, V.E. Exact Solutions of Bernoulli and Logistic Fractional Differential Equations with Power Law Coefficients. *Mathematics* **2020**, *8*, 2231. [CrossRef]
15. Abdeljawad, T.; Al-Mdallal, Q.M.; Jarad, F. Fractional logistic models in the frame of fractional operators generated by conformable derivatives. *Chaos Solitons Fractals* **2019**, *119*, 94–101. [CrossRef]
16. Cao, J.; Qiu, Y. A high order numerical scheme for variable order fractional ordinary differential equation. *Appl. Math. Lett.* **2016**, *61*, 88–94. [CrossRef]
17. Baskonus, H.M.; Bulut, H. On the numerical solutions of some fractional ordinary differential equations by fractional Adams-Bashforth-Moulton method. *Open Math.* **2015**, *13*. [CrossRef]
18. Li, C.; Zeng, F. The Finite Difference Methods for Fractional Ordinary Differential Equations. *Numer. Funct. Anal. Optim.* **2013**, *34*, 149–179. [CrossRef]
19. Li, C.; Chen, A.; Ye, J. Numerical approaches to fractional calculus and fractional ordinary differential equation. *J. Comput. Phys.* **2011**, *230*, 3352–3368. [CrossRef]
20. Diethelm, K.; Freed, A.D. The FracPECE subroutine for the numerical solution of differential equations of fractional order. *Forsch. Wiss. Rechn.* **1998**, *1999*, 57–71.
21. World Health Organization, Coronavirus Disease (COVID-19) Pandemic. Available online: <https://www.who.int/emergencies/diseases/novel-coronavirus-2019/events-as-they-happen> (accessed on 18 May 2021).
22. Zhang, Y.; Yu, X.; Sun, H.; Tick, G.R.; Wei, W.; Jin, B. Applicability of time fractional derivative models for simulating the dynamics and mitigation scenarios of COVID-19. *Chaos Solitons Fractals* **2020**, *138*, 109959. [CrossRef]
23. Kumar, P.; Erturk, V.S. The analysis of a time delay fractional COVID-19 model via Caputo type fractional derivative. *Math. Methods Appl. Sci.* **2020**. [CrossRef]

24. Alkahtani, B.S.T.; Alzaid, S.S. A novel mathematics model of covid-19 with fractional derivative. Stability and numerical analysis. *Chaos Solitons Fractals* **2020**, *138*, 110006. [[CrossRef](#)] [[PubMed](#)]
25. Torrealba-Rodriguez, O.; Conde-Gutiérrez, R.; Hernández-Javier, A. Modeling and prediction of COVID-19 in Mexico applying mathematical and computational models. *Chaos Solitons Fractals* **2020**, *138*, 109946. [[CrossRef](#)] [[PubMed](#)]
26. Sabatier, J.; Agrawal, O.P.; Machado, J.T. *Advances in Fractional Calculus*; Springer: Berlin/Heidelberg, Germany, 2007; Volume 4.
27. Baleanu, D.; Diethelm, K.; Scalas, E.; Trujillo, J.J. *Fractional Calculus: Models and Numerical Methods*; World Scientific: Singapore, 2012; Volume 3.
28. Diethelm, K.; Ford, N.J. Analysis of Fractional Differential Equations. *J. Math. Anal. Appl.* **2002**, *265*, 229–248. [[CrossRef](#)]
29. Li, C.; Chen, A. Numerical methods for fractional partial differential equations. *Int. J. Comput. Math.* **2017**, *95*, 1048–1099. [[CrossRef](#)]
30. Li, C.; Zeng, F. Finite Difference Methods for Fractional Differential Equations. *Int. J. Bifurc. Chaos* **2012**, *22*, 1230014. [[CrossRef](#)]
31. Coronavirus Resource Center. Available online: <https://coronavirus.jhu.edu/map.html> (accessed on 15 July 2021).
32. Suárez, V.; Quezada, M.S.; Ruiz, S.O.; Jesús, E.R.D. Epidemiología de COVID-19 en México: Del 27 de febrero al 30 de abril de 2020. *Rev. Clínica Española* **2020**, *220*, 463–471. [[CrossRef](#)]
33. COVID-19 Tablero México-CONACYT-CentroGeo-GeoInt-DataLab. Available online: <https://datos.covid-19.conacyt.mx/> (accessed on 18 May 2021).